NASA CONTRACTOR
REPORT

NASA CR-1364

NASA CR-13

C. 1

THE THIN FILM IRIS

by R. L. Ramey, H. S. Landes, and E. A. Manus

Prepared by
UNIVERSITY OF VIRGINIA
Charlottesville, Va.
for

NATIONAL AERONAUTICS AND SPACE ADMINISTRATION • WASHINGTON, D. C. • JUNE 1969

THE THIN FILM IRIS

By R. L. Ramey, H. S. Landes,
and E. A. Manus

Abstract

The introduction of thin conducting films into the fabrication of micro-
wave devices opens a new area of research and development. Because thin
conducting films have a finite conductivity (as contrasted to the almost
perfect conductivity of most bulk metals) they can support an electric
field. Thus the conventional boundary condition that the tangential
component of electric field strength is zero at a conducting surface does
not apply to these films with their finite conductivity.

In this paper the conventional theory of the waveguide iris is modified
to include this new boundary condition. As a direct result of this phenome-
non we find that the rectangular iris, which would normally be inductive,
is now capacitive under predictable conditions. Since the microwave im-
pedance behavior of thin films is now understood, it is possible to begin
a comprehensive study of the design of thin film active and passive micro-
wave devices.

THE THIN FILM IRIS

by

R.L. Ramey, H.S. Landes, and E.A. Manus
Department of Electrical Engineering
The University of Virginia

Summary

Because of the ability of a thin metallic film to support a tangential
component of electric field at its surface, it is possible to construct
microwave irises with these films which will display a capacitive reactance
where their exact counterpart constructed with a metal foil will appear as
an inductive reactance. A theoretical analysis of this effect is made and
the results compared to experimental observations.

Introduction

Interest in the possible application of thin film (less than 1000 Å)
microwave transmission windows as possible modulators or switches led to
the introduction of a very small iris in the film in order to both improve
the power transmission properties of the window and at the same time to
reduce the experimentally observed standing waves.

In each case the iris was carefully mounted in the transverse plane
of an X-band microwave system (Figure 1). The film or foil was connected
electrically to the walls of the waveguide by the use of conducting silver
paint. The dominant TE_{10} mode was employed and probing indicated that no
higher order modes could be detected. Table I compares similar irises
constructed from (a) nickel sheet 0.005 inches thick (127,000 angstroms)
and (b) a nickel film 475 angstroms thick which was deposited upon a
supporting mica substrate. Extensive tests have shown that mica substrates
several thousandths of an inch in thickness are transparent and do not
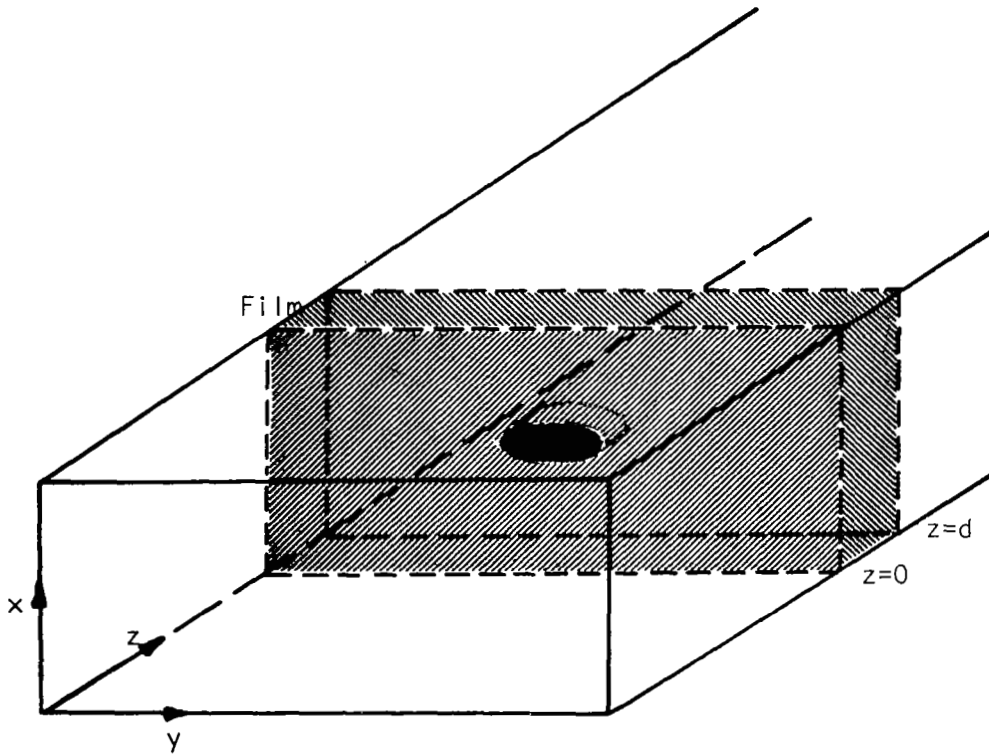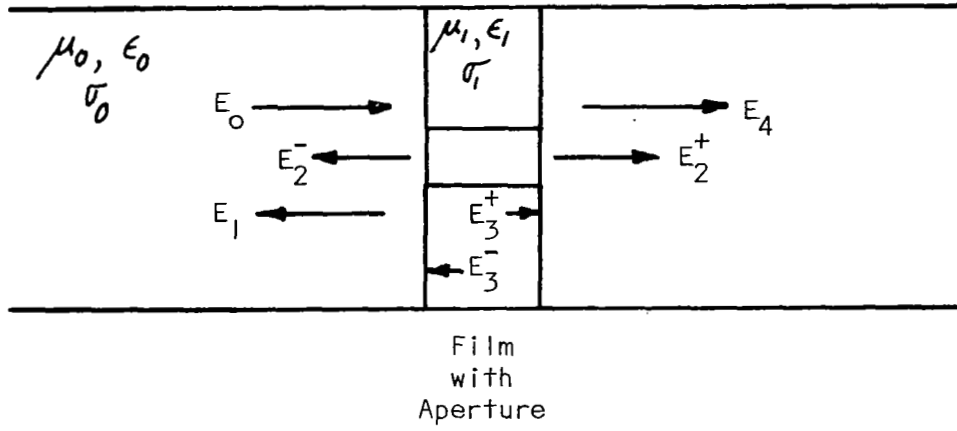
Figure 1. A Thin Film Waveguide Window
Which Contains an Aperture

reflect microwaves. This is not true for glass microscope slides which exhibit a pronounced reflection coefficient.

The comparison of the thin and thick film irises is very interesting and may be most readily seen on a Smith chart (Figure 2).

Although the experimental work involved only thin metallic films whose thickness is on the order of the carrier mean-free-path so that Fuchs-Sondheimer[1-5] theory applies and the conductivity of the film is finite and will support a tangential component of electric field at the film surface, this theory may also be applied to semiconducting films with certain restrictions that will be mentioned.

Diffraction by conventional screens, where the screen conductivity is essentially infinite, was first analyzed by Kirchhoff. Major improvements in the theory were made by H. Bethe[6] for the case of a single small aperture in a screen that has infinite conductivity. Although there has been some detailed discussion of Bethe's results for the near field,[7] his theory is generally accepted for far field calculations and will satisfy the usual waveguide measurement techniques. Extensive additions to diffraction theory have been made by Collin and Eggimann[8,9,10] and others[11] and we will find their work very helpful in refining the accuracy of our theoretical calculations. In reviewing these papers the reader should note that when a reference is made to a "thin diffraction film or screen" the papers are referring to the physical dimensions of the films in regard to the assumed boundary conditions and they are still assuming that the conductivity of their films is infinite.

Theory

With the assumption that the conductivity of our films is finite, we will proceed to analyze the case of a thin film diffraction screen that contains a single small hole and is mounted in the transverse plane of a rectangular waveguide as shown in Figure I. We will confine our analysis

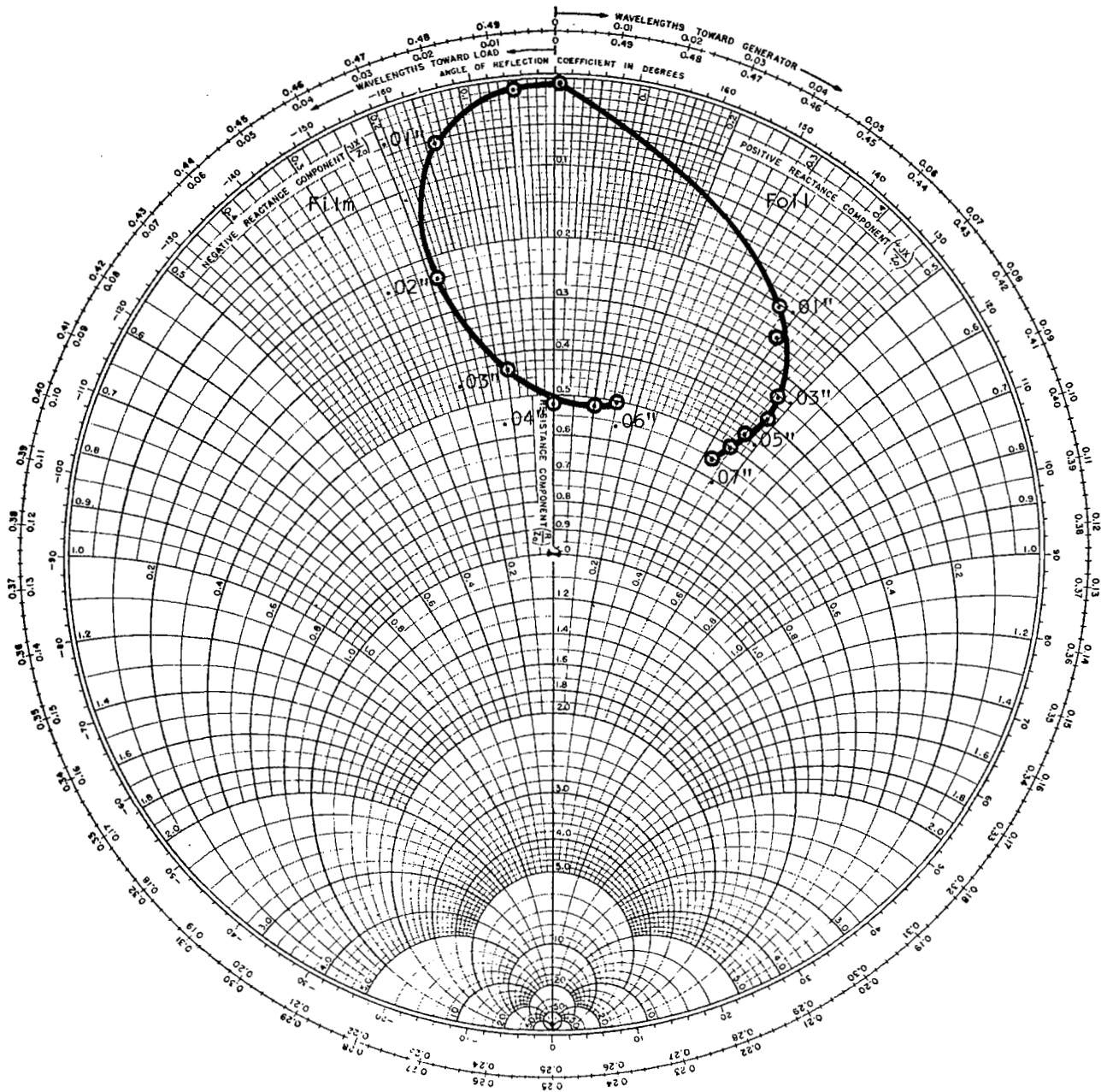Figure 2. A Smith Chart Plot of the Impedance of Two Similar Irises.
One made from a 475 angstrom nickel film and the other from
0.5 mil. nickel foil. In each case the rectangular aperture
was located at the center of the film and the length of the
aperture was held constant at 0.5 inches. The height of the
aperture was stepped from zero (no hole) up to 0.06 inches
for the film and 0.07 inches for the foil.

4

to the dominant TE_{10} mode. It is assumed that the incident wave $(\underset{\sim}{E}_0, \underset{\sim}{H}_0)$ is travelling in the $+z$-direction toward the front face of the film which is located at $z = 0$. Reflection from the film is usually relatively high and is represented by the wave $(\underset{\sim}{E}_1, \underset{\sim}{H}_1)$.

For sufficiently thin films[4] a measurable amount of energy in the wave (E_3^+, H_3^+) will penetrate the film. Some of this energy $(\underset{\sim}{E}_3^-, \underset{\sim}{H}_3^-)$ will be reflected from the far face of the film $(z = d)$ and the remainder will be transmitted entirely through the film $(\underset{\sim}{E}_4, \underset{\sim}{H}_4)$.

(A) NO HOLE IN FILM: In the absence of any hole in the film and with the film connected electrically to the surfaces of the waveguide, it has been shown that the transmission through any film is a function of the product of the film conductivity times the film thickness.[5] The power transmission coefficient is given by

$$T = \left| \frac{E_4}{E_0} \right|^2 = \left| \frac{2}{2 + \dfrac{\mu_o \gamma^2 d}{\mu \gamma_o}} \right|^2 \tag{1}$$

provided that $\gamma_o \ll \gamma$ and $\gamma_o d \ll 1$. The propagation factor is γ and μ is the permeability of the film. The permittivity of the film is ε. The subscript "0" designates free space values.

The propagation coefficient for the film is

$$\gamma = \left[\left(\frac{\pi}{a} \right)^2 - \omega^2 \mu \varepsilon + j \omega \mu \sigma \right]^{1/2} \tag{2a}$$

while for the free space in the waveguide it is

$$\gamma_o = \left[\left(\frac{\pi}{a} \right)^2 - \omega^2 \mu_o \varepsilon_o \right]^{1/2} \tag{2b}$$

The cutoff frequency for the dominant TE_{10} mode is obtained by setting $\gamma_o = 0$.

5

$$f_c^2 = \frac{1}{(2a)^2 \mu_o \varepsilon_o} \tag{3}$$

where a is the width of the waveguide. With this substitution Equation (2a) may be placed in the form:

$$\gamma = \left\{ \left(\frac{\pi}{a}\right)^2 \left[1 - \left(\frac{f}{f_c}\right)^2 \frac{\mu\varepsilon}{\mu_o \varepsilon_o}\right] + j\omega\mu\sigma \right\}^{1/2} \tag{4}$$

Substitution into Equation (1) yields a power transmission coefficient

$$T = \left| \frac{2}{2 - \dfrac{j\dfrac{f_c}{f}\left[\dfrac{\mu_o}{\mu} - \left(\dfrac{f}{f_c}\right)^2 \dfrac{\varepsilon}{\varepsilon_o}\right]\dfrac{\pi d}{a}}{\sqrt{1 - (f_c/f)^2}} + \dfrac{\sqrt{\mu_o/\varepsilon_o}\,\sigma d}{\sqrt{1 - (f_c/f)^2}}} \right|^2 \tag{5}$$

The imaginary term in the denominator is usually very small and may be neglected. A plot of

$$T = \left| \frac{2}{2 + \dfrac{\sqrt{\mu_o/\varepsilon_o}\,\sigma d}{\sqrt{1 - (f_c/f)^2}}} \right|^2 \tag{6}$$

is shown in Figure 3. Very good experimental verification of this relationship has been observed at 10 GHz for metal and semiconductor films.[5]

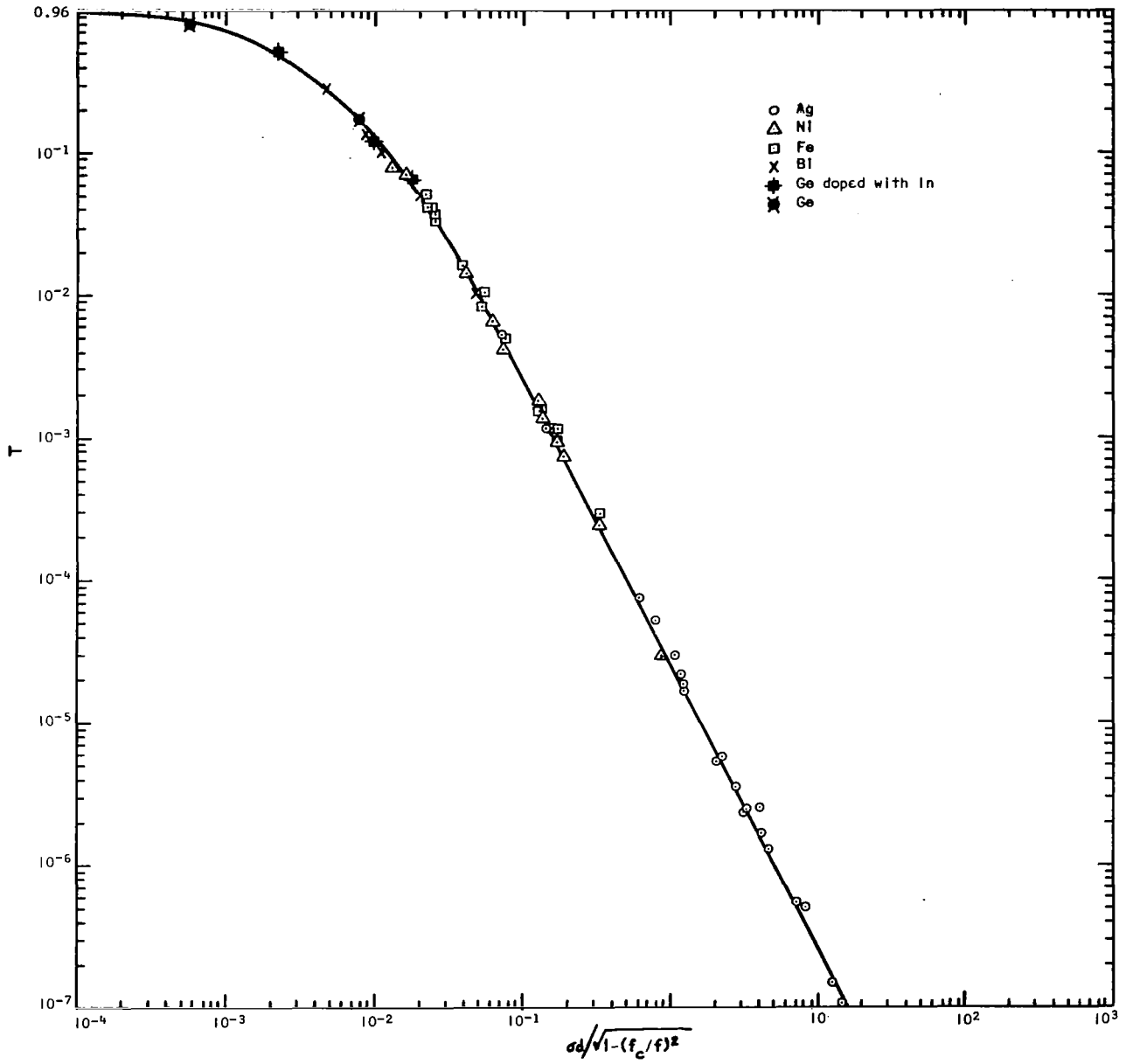The power reflection coefficient from a thin film is given by[4]

Figure 3. The Power Transmission of Thin Film Windows in Waveguide as a Function of σd

$$R_O = \left|\frac{E_1}{E_0}\right|^2 = \left|\frac{-\dfrac{\sqrt{\mu_O/\varepsilon_O}\ \sigma d}{2\sqrt{1-(f_c/f)^2}}}{1+\dfrac{\sqrt{\mu_O/\varepsilon_O}\ \sigma d}{2\sqrt{1-(f_c/f)^2}}}\right|^2 \tag{7}$$

$$R_O = |\Gamma_O|^2 \tag{8}$$

when Γ_O is the amplitude reflection coefficient and the impedance of free space is $\sqrt{\mu_O/\varepsilon_O} = 377$ ohms. A plot of Equation (8) is shown in Figure 4.

(B) DIFFRACTION HOLE IN FILM: A small hole whose radius, s, is much less than the guide wavelength of the incident EM wave is now located at the center of the film. The total power reflected and transmitted will be different from the previous case where there was no hole in the film. Bethe has shown that the effect of the hole may be taken into account by considering induced electric and magnetic dipoles to exist in the hole. As we are only interested in the far field results, we will follow a development similar to that used by Bethe but with the significant difference that the finite conductivity of our films permit us to have a tangential component of E_0 at the surface of the film whereas Bethe could not because he assumed a perfect conducting screen.

Let the total EM field developed by both oscillating dipoles be (E_2, H_2). Half of the energy radiated by the dipoles will be in a wave (E_2^-, H_2^-) travelling from the film toward the generator and the other half of the energy will be in the wave (E_2^+, H_2^+) that travels beyond the film. In the most general case
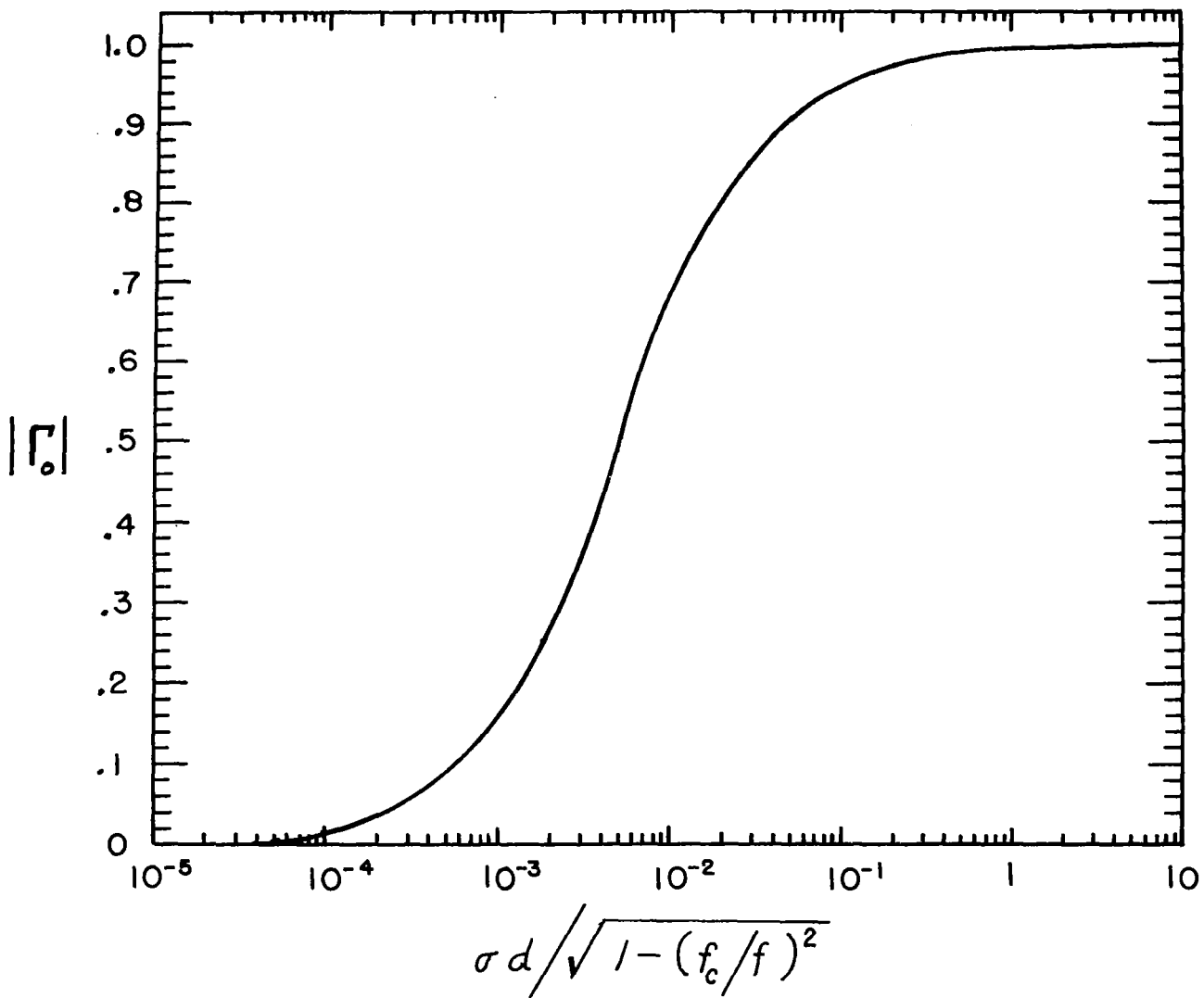
$$E_2 = E_p + E_m \tag{9}$$

8

Figure 4. The Magnitude of the Voltage Reflection Coefficient for Thin Film Windows in Waveguide

9

and

$$H_2 = H_p + H_m \tag{10}$$

where the wave (E_p, H_p) is generated by the induced, oscillating <u>electric dipole</u> located in the hole and the wave (E_m, H_m) is generated by the induced oscillating <u>magnetic dipole</u> that is located in the hole. Both of these dipoles are induced by the net fields at the film surface. That is, for the oscillating electric dipole:

$$\text{Wave } (E_p, H_p) = f(E_{0+} + E_{1+}) = f(E_{0+}[1 + \Gamma_o]) \tag{11}$$

and for the oscillating magnetic dipole:

$$\text{Wave } (E_m, H_m) = f(H_{0+} + H_{1+}) = f(H_{0+}[1 - \Gamma_o]) \tag{12}$$

In these equations, Γ_o is the amplitude reflection coefficient for the film without a hole. Specifically $\Gamma_o = E_{1+}/E_{0+} = -H_{1+}/H_{0+}$. Figure 5 is a sketch of the induced dipoles for the TE_{10} mode of excitation of the waveguide.

In the case of the induced electric dipole, only a tangential component of the original field can induce a dipole which, in turn, will radiate down the waveguide. Thus, when the diffraction screen has a finite conductivity, a tangential component of electric field $(E_{0+} + E_{1+})$ may exist at the screen and an oscillating electric dipole will be induced in the hole. Therefore, this analysis will differ from that of Bethe and others in that two additional terms may now exist in rectangular waveguides that have been previously ruled out by the infinite conductivity of the diffraction screens employed. First, for very thin films the direct transmission wave (E_4, H_4) may make a significant contribution. Second, an even more interesting term is the presence of the (E_p, H_p) wave radiated by the induced electric dipole. This wave has a pronounced effect upon the impedance presented by this
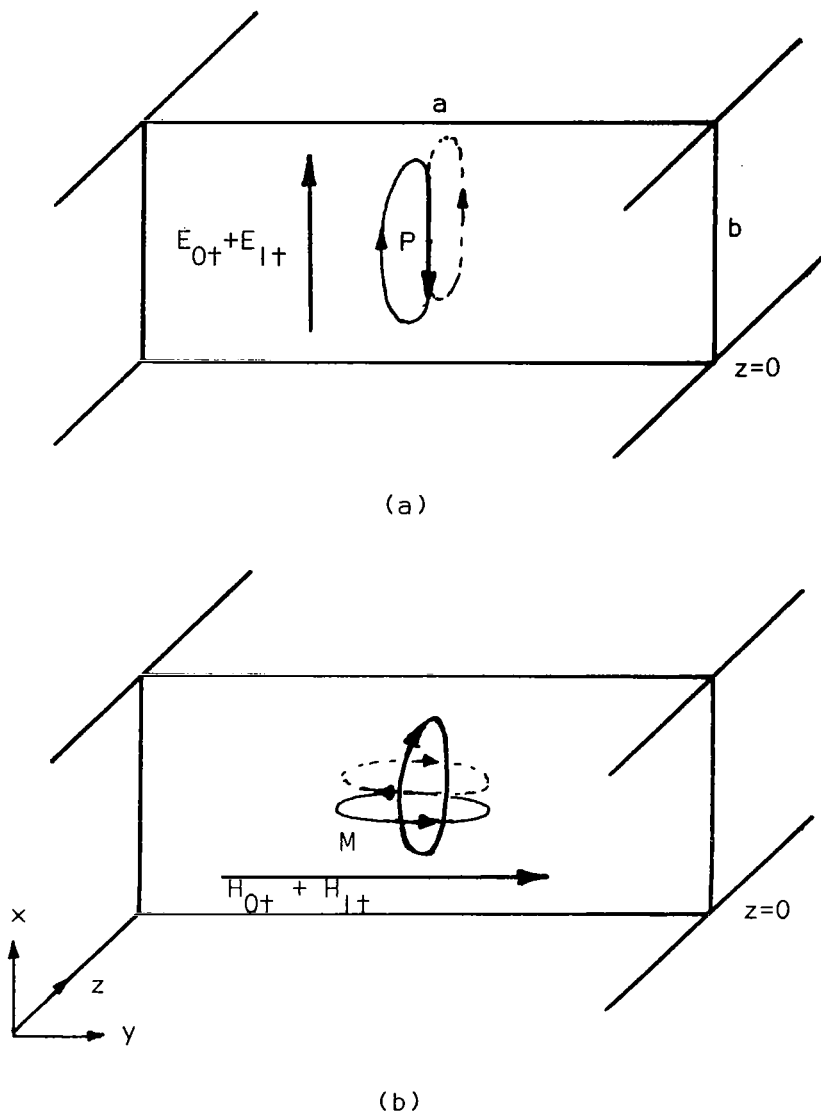
(a)

(b)

Figure 5. Sketches of the Induced Electric (a) and
Magnetic (b) Dipoles Which Represent the
Reactance of the Aperture

11

diffraction screen or iris in the waveguide.

Boundary conditions for only the tangential components of the electric field are sufficient when the analysis is limited to the TE_{10} mode. The continuity of tangential components over the left hand surface ($z = 0$) of the film permits us to write

$$\underset{\sim}{E}_{0t} + \underset{\sim}{E}_{1t} = \underset{\sim}{E}(0)_{Film\ t} = \underset{\sim}{E}_{3t}^{+}(0) + \underset{\sim}{E}_{3t}^{-}(0) \qquad (film) \qquad (13)$$

while at the right hand surface ($z = d$) we have

$$\underset{\sim}{E}_{4t} = \underset{\sim}{E}(d)_{Film\ t} = \underset{\sim}{E}_{3t}^{+}(d) + \underset{\sim}{E}_{3t}^{-}(d) \qquad (film) \qquad (14)$$

The continuity of tangential components <u>over the surface of the hole</u> leads to

$$\underset{\sim}{E}_{0t} + \underset{\sim}{E}_{1t} + \underset{\sim}{E}_{2t}^{-} = \underset{\sim}{E}_{4t} + \underset{\sim}{E}_{2t}^{+} \qquad (hole) \qquad (15)$$

and

$$\underset{\sim}{H}_{0t} + \underset{\sim}{H}_{1t} + \underset{\sim}{H}_{2t}^{-} = \underset{\sim}{H}_{4t} + \underset{\sim}{H}_{2t}^{+} \qquad (hole) \qquad (16)$$

where we are assuming that the film is sufficiently thin so that there is negligible variation in any of these fields as we pass through the hole. Thus, the theory being developed here may also be applied to any semiconducting sample provided that the above assumption is valid. Because of the relatively low conductivity of semiconductors there is a tendency to use wafers instead of thin films and hence the preceding caution is of importance.

The radiation from the dipole, on each side of the iris, is equal in magnitude and differs only in the direction of propagation. Thus

$$\underset{\sim}{E}_{2t}^{-} = \underset{\sim}{E}_{2t}^{+} \qquad (hole) \qquad (17)$$

and

$$H_{2t}^- = - H_{2t}^+ \qquad \text{(hole)} \qquad (18)$$

If we substitute Equations (17) and (18) into Equations (15) and (16) we obtain

$$E_{0t} + E_{1t} = E_{4t} \qquad \text{(hole)} \qquad (19)$$

$$H_{0t} + H_{1t} - H_{4t} = 2H_{2t}^+ \qquad \text{(hole)} \qquad (20)$$

Following Collin's general approach,[12,13] we will express the fields radiated by the dipoles in terms of scattering coefficients and the excitation fields. With reference to Equations (9) and (10) as well as (11) and (12) we may write

$$E_{2t}^- = \psi_{11}(E_{0t} + E_{1t}) + \psi_{12}(H_{0t} - H_{1t})$$

$$= \psi_{11}(1 + \Gamma_o) E_{0t} + \psi_{12}(1 - \Gamma_o)H_{0t} \qquad (21)$$

$$H_{2t}^- = + \psi_{21}(E_{0t} + E_{1t}) + \psi_{22}(H_{0t} - H_{1t})$$

$$= + \psi_{21}(1 + \Gamma_o)E_{0t} + \psi_{22}(1 - \Gamma_o)H_{0t} \qquad (22)$$

where the ψ's are the scattering coefficients.

It is convenient to include the reflection coefficient, Γ_o, in the scattering coefficient. Also, in the case of the dominant TE_{10} mode, the electric field is proportional to the magnetic field and we may write:

$$E_{2t}^- = (\psi_p + \psi_m)E_{0t} = \psi E_{0t} \qquad (23)$$

$$H_{2t}^- = (\psi_p + \psi_m)H_{0t} = \psi H_{0t} \qquad (24)$$

13

where the scattering coefficient ψ_p applies to the EM field produced by the oscillating electric dipole and ψ_m applies to the field produced by the oscillating magnetic dipole. Either one of these equations contains all the information we require.

The scattering coefficients may be found by utilizing the Lorentz reciprocity theorem which in general relates two current sources J_f and J_g and their respective fields E_f, H_f and E_g, H_g according to

$$\int_S (E_f \times H_g - E_g \times H_f) \cdot n dS = \int_V (E_g \cdot J_f - E_f \cdot J_g) dV \qquad (25)$$

where n is the outward normal unit vector to the surface enclosing the sources.

The scattering coefficients will be derived in terms of unit amplitude fields. Then E_{0+} in Equation (23) will determine the amplitude of E_{2+}^-. Lower case letters will represent normalized quantities. In our problem only a single source exists in the volume, V, which is positioned so as to include the film. See Figure 6. Then J_g in Equation (25) is zero and J_f radiates the wave e_f, h_f which is due to the oscillating magnetic and electric dipoles located at the iris. The volume must be large enough so that only dominant mode operation will exist outside the volume. Thus, the planes located at z_a and z_b will each to several wavelengths from the radiating dipoles. The normalized fields excited by the dipoles are assumed to be of the dominant TE_{10} mode when measured beyond the planes $z = z_a$, z_b and are designated by e_g and h_g. In general:
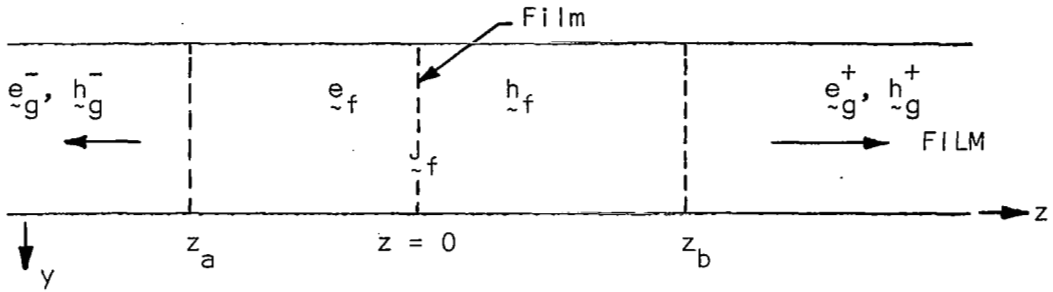
Figure 6. A Current Source in the Volume Bounded by the Waveguide and the planes z_a, z_b

$$e_f^+ = \psi^+ e_{fx}\underset{\sim}{i} \qquad\qquad (26a)$$

$$h_f^+ = \psi^+(h_{fy}\underset{\sim}{j} + h_{fz}\underset{\sim}{k}) \qquad\qquad (26b)$$

$$e_f^- = \psi^- e_{fx}\underset{\sim}{i} \qquad\qquad (26c)$$

$$h_f^- = \psi^-(- h_{fz}\underset{\sim}{j} + h_{fz}\underset{\sim}{k}) \qquad\qquad (26d)$$

The wave e_g^-, h_g^- propagated in the negative z - direction is

$$e_g^- = e_{gx}\underset{\sim}{i} \qquad\qquad (27a)$$

$$h_g^- = h_{gy}\underset{\sim}{j} + h_{gz}\underset{\sim}{k} \qquad\qquad (27b)$$

and Equation 25 becomes

15

$$\int_{z_b} [\psi^+ e_{fx}\underset{\sim}{i} \times(- h_{gy}\underset{\sim}{j} + h_{gz}\underset{\sim}{k}) - \psi^+ e_{gx}\underset{\sim}{i} \times(h_{fy}\underset{\sim}{j} + h_{fz}\underset{\sim}{k})] \cdot \underset{\sim}{k} dS$$

$$+ \int_{z_a} [\psi^- e_{fx}\underset{\sim}{i} \times(- h_{gy}\underset{\sim}{j} + h_{gz}\underset{\sim}{k}) - \psi^- e_{gx}\underset{\sim}{i} \times(- h_{fy}\underset{\sim}{j} + h_{fz}\underset{\sim}{k}) \cdot (-\underset{\sim}{k}) dS$$

$$= \int_V \underset{\sim}{e}_g^- \cdot \underset{\sim}{J}_f dV \tag{28}$$

The waveguide walls are considered to be perfect conductors and therefore the wall surface integrals are zero. Thus, Equation (28) reduces to

$$- \int_{z_b} \psi^+ [e_{fx}h_{gy} + e_{gx}h_{fy}] dS + \int_{z_a} \psi^- [e_{fx}h_{gy} - e_{gx}h_{fy}] dS$$

$$= \int_V \underset{\sim}{e}_g^- \cdot \underset{\sim}{J}_f dV \tag{29}$$

Now at the surfaces $z = z_a$ and $z = z_b$ we are assuming that the fields radiated by the dipoles have become TE_{10} modes and therefore

$$e_{fx} = e_{gx} = e_x \quad \text{for } z = z_a, \ z_b \tag{30}$$

and

$$h_{fy} = h_{gy} = h_y \quad \text{for } z = z_a, \ z_b \tag{31}$$

With these substitutions we may solve for the scattering coefficient ψ^+ in Equation (29).

$$\psi^+ = - \frac{1}{2 S_o} \int_V \underset{\sim}{e}_g^- \cdot \underset{\sim}{J}_f dV \tag{32}$$

where

$$S_o = \int_o^b \int_o^a e_x h_y dS \quad \text{for } z = z_b \tag{33}$$

16

The current source, $\underset{\sim}{J}_f$, may be represented by a current loop in the xz-plane and an x-directed electric current element in the xy-plane as shown in Figure 5. Let us consider the current loop first. If the radius of the loop, $s \ll \lambda_g$ then the magnetic flux density is approximately constant over the loop area. By Equation (32)

$$\underset{\sim}{\psi}_m^+ = - \frac{1}{2S_o} \int_\ell \underset{\ell\sim g}{e} \cdot I\ell d\ell$$

$$= - \frac{I}{2S_o} \int_A \nabla\times \underset{\sim}{e}_g^- \cdot \underset{\sim}{n} dA \tag{34}$$

where the surface unit vector $\underset{\sim}{n} = \underset{\sim}{j}$ and the subscript, m, has been introduced to signify that this scattering coefficient is arising from a magnetic dipole.

$$\nabla \times \underset{\sim g}{e}^- = - j\omega\mu_o \underset{\sim g}{h}^- \tag{35}$$

in accord with Maxwell's equations for a TE_{10} mode. Then

$$\psi_m^+ = \frac{j\omega I}{2S_o} \int_A \mu_o \underset{\sim g}{h}^- \cdot \underset{\sim}{n} dA \tag{36}$$

According to Equation (27b)

$$\underset{\sim g}{h} \cdot \underset{\sim}{j} = h_{gy}$$

which may be written as

$$h_{gy} = - \frac{\beta}{\omega\mu_o} \sin \frac{\pi y}{a} \tag{37}$$

where $\beta = \omega \sqrt{\mu_o \epsilon_o} [1 - (f_c/f)^2]^{1/2}$. If we evaluate this expression for

17

h_{gy} at the center of the iris ($y = a/2$) we find that

$$h_{gy} = -\frac{\beta}{\omega\mu_o} \tag{38}$$

With these substitutions

$$\psi_m^+ = -\frac{j\beta M_y}{2S_o} \tag{39}$$

where $M_y = IA$ is the y-directed magnetic dipole.

The dipole moment for radiation in the $-z$ direction may be written as

$$M_y = \alpha_m(-h_y) \tag{40}$$

where α_m is the magnetic polarizability of the aperture

Normalize the fields relative to $|E_{0+}|$. Thus from Equations (13) and (16) we have for the normalized fields

$$\underset{\sim}{e}_{0+} + \underset{\sim}{e}_{1+} = e_x\underset{\sim}{i} = [\exp(-j\beta z) + \Gamma_o \exp(j\beta z)]\sin\frac{\pi y}{a}\underset{\sim}{i} \tag{41a}$$

$$\underset{\sim}{h}_{0+} + \underset{\sim}{h}_{1+} = h_y\underset{\sim}{j} = \frac{\beta}{\omega\mu_o}[\exp(-j\beta z) - \Gamma_o \exp(j\beta z)]\sin\frac{\pi y}{a}\underset{\sim}{j} \tag{41b}$$

By Equation (41b) the normalized magnetic field at the center of the aperture is

$$h_y = \frac{\beta}{\omega\mu_o}(1 - \Gamma_o) \tag{42}$$

However, the dipole moment must be doubled to take into account its minor image in the film plane because we must remember that <u>in our physical</u>

18

model there is no hole in the film. The area

$$S_o = \int_o^b \int_o^a \frac{\beta}{\omega\mu_o} \sin^2 \frac{\pi y}{a} \, dy \, dx$$

$$= \frac{ab\beta}{2\omega\mu_o} \tag{43}$$

Substituting, we obtain

$$\psi_m^+ = \frac{j2\alpha_m \beta(1 - \Gamma_o)}{ab} \tag{44}$$

A similar treatment using the wave $\underset{\sim}{e}_g^+$, $\underset{\sim}{h}_g^+$ in the reciprocity theorem leads to the result that

$$\psi_m^- = \psi_m^+ \tag{45}$$

Thus far we have ignored the electric current element that appeared in Equation (32). An oscillating current element may be represented by an electric dipole which can exist in the plane of the aperture because the film is not a perfect conductor. Using Equation (36)

$$\psi_p^+ = - \frac{1}{2S_o} \int_V \underset{\sim}{\varepsilon}_x^i \cdot \underset{\sim}{J}_f \, dV$$

$$= - \frac{1}{2S_o} \underset{\sim}{\varepsilon}_x^i \cdot j\omega I d\ell \underset{\sim}{i}$$

$$= - \frac{1}{2S_o} \underset{\sim}{\varepsilon}_x^i \cdot j\omega \underset{\sim}{P} \tag{46}$$

The electric dipole moment is

$$\underset{\sim}{P} = - \varepsilon_o \alpha_e \underset{\sim}{e}_x^i \tag{47}$$

where α_e is the electric polarizability of the aperture. From Equation (41a), evaluated at $y = 1/2a$,

$$e_x = 1 + \Gamma_o \tag{48}$$

19

Substituting we have

$$\psi_p^+ = \frac{-j\alpha_e \omega^2 \epsilon_o \mu_o (1 + \Gamma_o)}{ab\beta} \tag{49}$$

The subscript p is introduced to identify the scattering coefficient with the electric dipole. The dipole moment and the excitation wave are the same for the scattering coefficient in the region z < 0. Therefore

$$\psi_p^+ = \psi_p^- \tag{50}$$

Equations (23) and (24) may now be written

$$E_{2t}^- = E_{2x}^- = (\psi_p^- + \psi_m^-)A \sin \frac{\pi y}{a} e^{j\beta z} \tag{51a}$$

$$E_{2t}^+ = E_{2x}^+ = (\psi_p^+ + \psi_m^+)A \sin \frac{\pi y}{a} e^{-j\beta z} \tag{51b}$$

$$H_{2t}^- = H_{2y}^- = -(\psi_p^- + \psi_m^-)A \frac{\beta}{\omega\mu_o} \sin \frac{\pi y}{a} e^{j\beta z} \tag{51c}$$

$$H_{2t}^+ = H_{2y}^+ = (\psi_p^+ + \psi_m^+)A \frac{\beta}{\omega\mu_o} \sin \frac{\pi y}{a} e^{-j\beta z} \tag{51d}$$

where

$$E_{0t} = E_{0x} = A \sin\frac{\pi y}{a} e^{-j\beta z} \tag{52a}$$

$$H_{0t} = H_{0y} = A \frac{1}{Z_\omega} \sin \frac{y}{a} e^{-j\beta z} \tag{52b}$$

The scattering coefficients may be evaluated upon selecting applicable electric and magnetic polarizabilities, α_e and α_m, for a particular aperture configuration. Exact values for elliptical configurations and approximate

values for slots may be found in the literature[14,15].

From impedance measurements on bulk and thin film screens with identical apertures effective values of α_e and α_m may be determined for any aperture configuration whose dimensions are small with respect to the wavelength.

The **power transmission coefficient** for a thin film screen that contains an aperture is

$$T = \left| \frac{E_{4+} + E^+_{2+}}{E_{0+}} \right|^2 \qquad (TE_{10} \text{ mode}) \tag{53}$$

which may be written in the form

$$T = \left| T_o^{1/2} + T_h^{1/2} \right|^2 \tag{54}$$

where T_o is the power transmission through the film when there is no aperture (Equation (6)) and $T_h = \left| E^+_{2+}/E_{0+} \right|^2$ is the power transmission through the aperture. In the case of the thicker films, T_o will be insignificant and T_h will be the important term. By Equation (17),

$$T_h = \left| \frac{E^+_{2+}}{E_{0+}} \right|^2 = \left| \frac{E^-_{2+}}{E_{0+}} \right|^2 \tag{55}$$

Substituting the appropriate values for the scattering coefficients, the power transmission of the iris is

$$T_h = \left| \psi_p + \psi_m \right|^2 \tag{56}$$

The **power reflection coefficient** for an iris for the TE_{10} mode is obtained in a similar manner:

21

$$R = \left| \frac{E_{1t} + E_{2t}^-}{E_{0t}} \right|^2 = \left| R_o^{1/2} + R_h^{1/2} \right|^2 \qquad (57)$$

Where R_o is the power reflection coefficient for the thin film without a hole and $R_h = |E_{2t}^-/E_{0t}|^2 = T_h$ is the power reflection coefficient of the hole alone and is equal to the power transmission coefficient of the hole. As the power absorption coefficient, A_h, of the hole is zero, it follows from the general relationship between the power coefficients:

$$T_h + R_h + A_h = 1 \qquad (58)$$

that $T_h = R_h = \frac{1}{2}$. If we substitute Equation (23) into Equation (57) we obtain

$$R = |\Gamma_o + \psi_p + \psi_m|^2 \qquad (59)$$

The _impedance of the iris_ is of special interest, particularly when we compare its impedance to that of a similar iris constructed of a thick film ($\rho \approx 0$). The impedance of the waveguide system, at any point, $z < 0$, is (TE_{10} mode):

$$Z = \frac{E_t}{H_t} = \frac{E_{0t} + E_{1t} + E_{2t}^-}{H_{0t} + H_{1t} + H_{2t}^-} = \left(\frac{E_{0t}}{H_{0t}} \right) \frac{1 + \frac{E_{1t}}{E_{0t}} + \frac{E_{2t}^-}{E_{0t}}}{1 + \frac{H_{1t}}{H_{0t}} + \frac{H_{2t}^-}{H_{0t}}} \qquad (60)$$

Introduce the amplitude reflection coefficient for a film without a hole, $\Gamma_o = E_{1t}/E_{0t} = -H_{1t}/H_{0t}$ and also the amplitude reflection coefficient for the hole, $E_{2t}^-/E_{0t} = -H_{2t}^-/H_{0t}$ and Equation (60) becomes

$$Z = Z_o \frac{1 + \Gamma_o + (\psi_p + \psi_m)}{1 - \Gamma_o - (\psi_p + \psi_m)} \qquad (61)$$

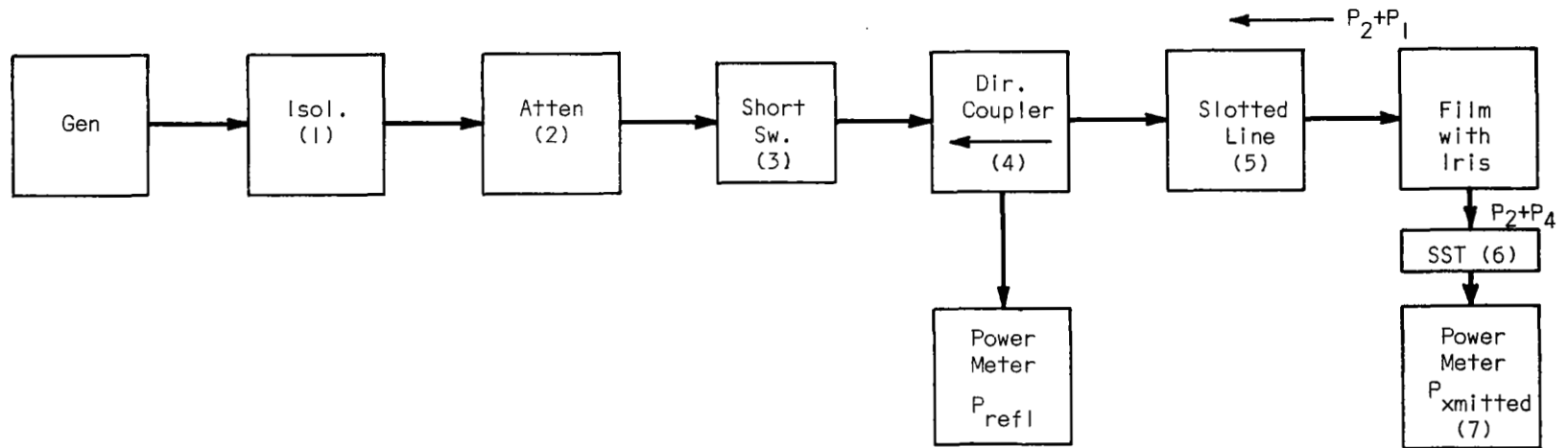where Z_o is the characteristic impedance of the waveguide.

22

Experimental Verification

The preceding analysis may be verified by experimental observations. The reactance of any iris may be calculated provided that the proper polarizability of the aperture may be ascertained. The calculation of polarizabilities for circular, elliptical, and rectangular apertures is discussed in the Appendix. The general microwave layout is shown in Figure 7. It is important to maintain very small standing wave ratios if power measurement errors are to be minimized.

The results of the measurements made on an iris, manufactured from a nickel film 280 angstrons thick which was vacuum deposited on a mica substrate, is shown in Table I. First, a circular aperture was made by carefully shaving off the unwanted film. Measurements were made and then the aperture was enlarged to an ellipse with a minor axis $\ell_x = \frac{1}{2}(0.1)$ inches and a major axis $\ell_y = \frac{1}{2}(0.25)$ inches. After each set of microwave measurements the elliptical aperture was enlarged as tabulated.

With reference to the Appendix, the electric and magnetic polarizations as a function of the eccentricity of each elliptical aperture were computed. From this information the impedance of each iris was computed and compared with the measured values as shown in Figure 8. Bearing in mind the simplicity of our model for the aperture and the restriction to "small holes", the results are very encouraging. Better correlation between the calculated and measured resistances is desirable and we are making some improvements along this line which will be discussed in a subsequent report.

It is important to note that none of the elliptical apertures displayed a capacitive reactance. Yet comparable rectangular apertures in thin films do display a capacitive reactance (See Figure 2) provided the minor axis is kept relatively small. This observation was verified on other films and it was found that the rounded corners of the elliptical aperture in the thin film of finite conductivity played an important role

$\xleftarrow{\hspace{1cm}} P_2 + P_1$

```
┌──────┐      ┌──────┐      ┌──────┐      ┌──────┐      ┌──────┐      ┌──────┐      ┌──────┐
│      │      │      │      │      │      │Short │      │ Dir. │      │      │      │ Film │
│ Gen  │─────>│ Isol.│─────>│Atten │─────>│ Sw.  │─────>│Coupler│────>│Slotted│────>│ with │
│      │      │ (1)  │      │ (2)  │      │ (3)  │      │ <──  │      │ Line │      │ Iris │
│      │      │      │      │      │      │      │      │ (4)  │      │ (5)  │      │      │
└──────┘      └──────┘      └──────┘      └──────┘      └──────┘      └──────┘      └──────┘
```

$P_2 + P_4$

```
                                                            │                          │
                                                            v                      ┌────────┐
                                                        ┌──────┐                   │ SST (6)│
                                                        │Power │                   └────────┘
                                                        │Meter │                        │
                                                        │      │                        v
                                                        │Prefl │                   ┌────────┐
                                                        └──────┘                   │ Power  │
                                                                                   │ Meter  │
                                                                                   │Pxmitted│
                                                                                   │  (7)   │
                                                                                   └────────┘
```

(1) Isolator   SWR < 1.2
(2) Attenuator   SWR < 1.15
(3) Switch   SWR < 1.10
(4) Directional Coupler SWR < 1.10
(5) Slotted Line   SWR < 1.20
(6) Slide Screw Tuner
(7) Power Meter   SWR < 1.02

Figure 7. The General Experimental Arrangements Used at 10 Ghz

TABLE I

NICKEL FILM IRIS

TRIAL	CONFIGURATION	$\bar{P_2}+P_4$	SWR	MIN.	$\Delta\lambda_g$	z	$P_{reflected}$	$P_{absorbed}$
	REFERENCE	10mω	1.005	14.95				
	SOLID	17.3μω	40	−.003	.00073	.03 − j0+	9.04	.96
	$2\ell_x=2\ell_y=0.1$	22μω	32	+.003	.00073	.032 + j0+	8.82	1.18
1	$2\ell_x=.1$ $2\ell_y=.25$	.123mω	21.8	+.024	.00585	.048 +j.032	8.32	1.56
2	$2\ell_x=.1$ $2\ell_y=.281$	.281mω	16.1	+.035	.0085	.06 +j.055	7.80	1.92
3	$2\ell_x=.1$ $2\ell_y=.343$	.575mω	11.85	+.058	.0141	.088 +j.09	7.13	2.25
4	$2\ell_x=.1$ $2\ell_y=0.438$	2.15m	4.37	+.105	.0256	.232 +j.155	3.94	3.90
5	$2\ell_x=.1$ $2\ell_y=.5$	4.20m	2.23	+.052	.0127	.44 +j.07	1.45	4.30
6	$2\ell_x=.1$ $2\ell_y=.625$	5.25	2.33	−.195	.0476	.455 −j.242	1.59	3.16

d = 280 angstrons

$\dagger$d = 25 × 10^{-3}

From Figure 4:
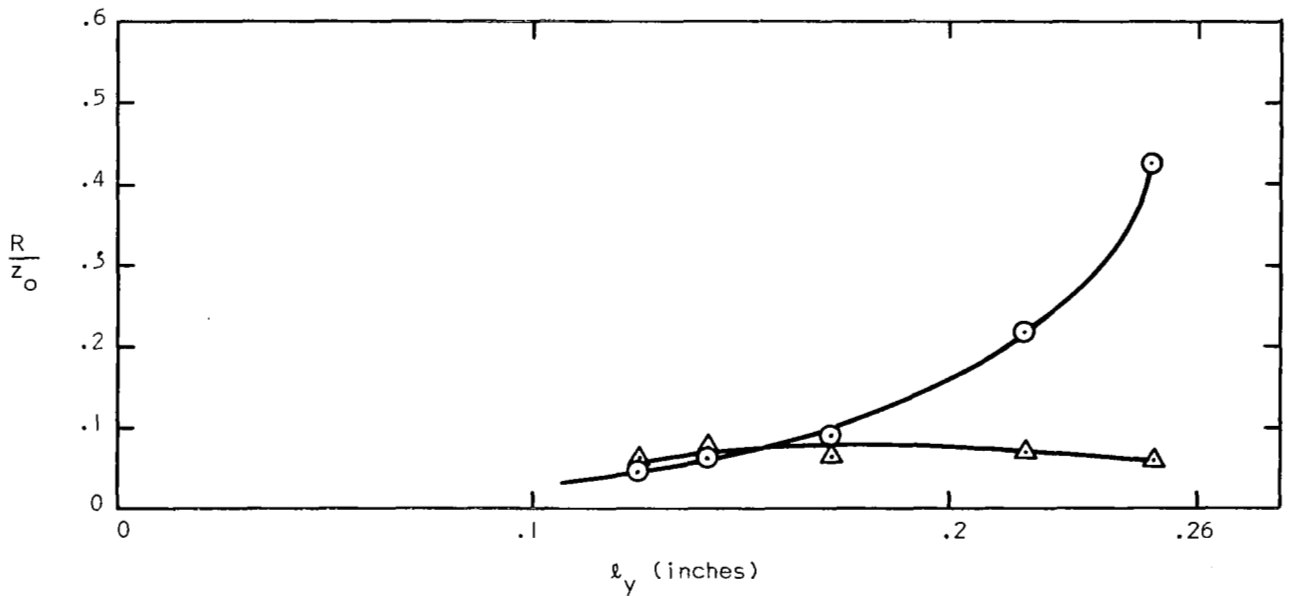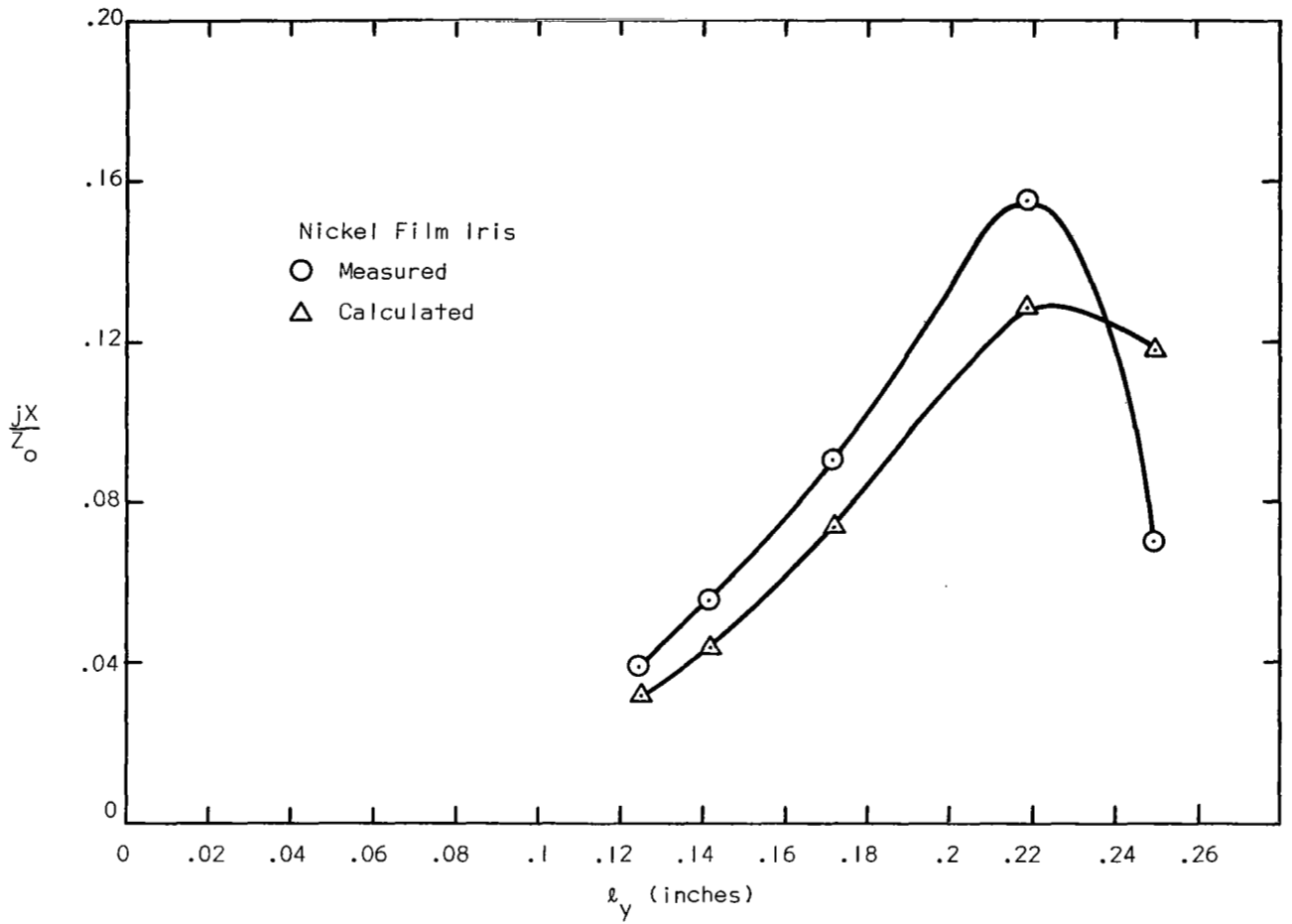
$\Gamma_o = 0.88$

25

Figure 8. A Comparison of the Calculated and Measured Reactances and Resistances for the Elliptical Apertures Tabulated in Table I.

26

in controlling the reactance of the iris. This suggests many interesting microwave circuit possibilities and we are therefore exploring this phenomenon in more detail. In particular we require a suitable theoretical expression for the polarizability of the rectangular aperture and we are working toward this goal. In the meantime we have plotted empirical values of the polarizabilities of the rectangular aperture in Figure IA in the Appendix.

A comparison of the experimental and theoretical values of reactance and resistance for circular apertures is shown in Figure 9. The correlation between calculated and computed values of reactance is very good and the calculated values of resistance are of acceptable accuracy although improvements in the theory in regard to the dissipation in the iris are desirable.

Conclusions

The thin film iris can be designed to present either an inductive or a capacitive reactance whereas the conventional iris tends to be only inductive unless the aperture is extremely large. The theory developed here is adequate for describing this phenomenon and therefore we are in a position to proceed with the design of both passive and active microwave devices.
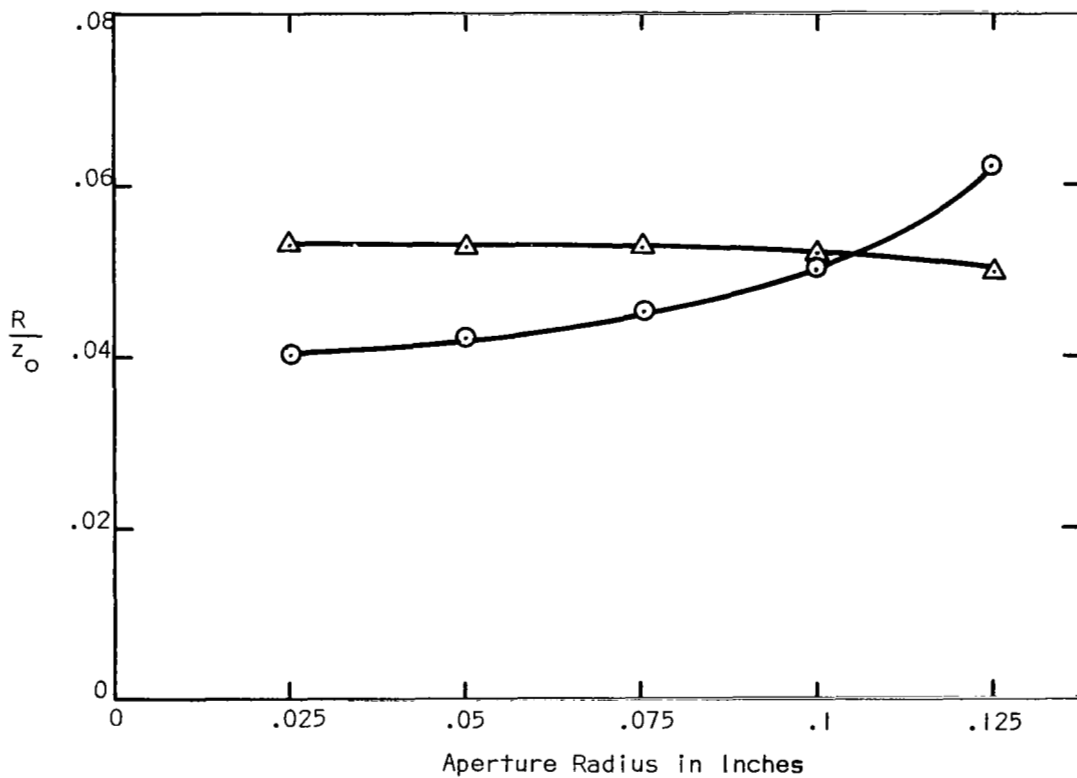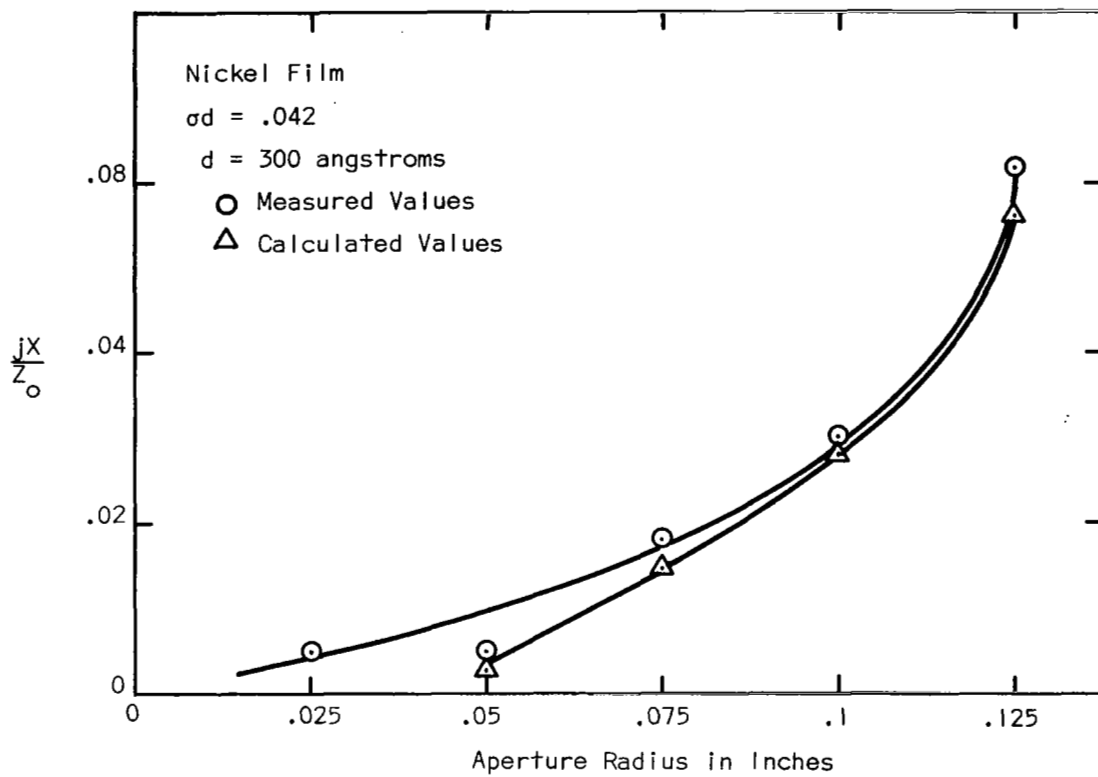
Figure 9. A Circular Aperture in a Nickel Film

28

Appendix

Calculation of the Scattering Coefficients, ψ_m and ψ_p for the Elliptical
Aperture

From Equations (44) and (49) the magnetic and electric scattering coefficients
are

$$\psi_m = \frac{j2\beta}{ab} \alpha_m (1 - \Gamma_o) \qquad\qquad\qquad (1A)$$

and

$$\psi_p = \frac{-j\omega^2 \mu_o \epsilon_o}{ab\beta} \alpha_e (1 + \Gamma_o) \qquad\qquad\qquad (2A)$$

$$\omega = 2\pi \times 9.8 \times 10^9 = 6.154 \times 10^{10} \text{ rad/sec}$$

$$a = .9 \times .0254 = 0.02286 \text{ meter}$$

$$b = .4 \times .0254 = 0.01016 \text{ meter}$$

$$f_c = 6.558 \text{ GHz.}$$

The phase constant is

$$\beta = \omega\sqrt{\mu_o \epsilon_o} \left[1 - (\frac{f_c}{f})^2\right]^{1/2} \qquad\qquad\qquad (3A)$$

Its value at 9.8 GHz is

$$\beta = \frac{6.154 \times 10^{10}}{3 \times 10^8} \left[1 - \frac{6.558}{9.80})^2\right]^{1/2}$$

$$= 152.4 \text{ rad/in.}$$

With these substitutions Equations (1A) and 2A) become:

$$\psi_m = j\ 1.312 \times 10^6\ \alpha_m (1 - \Gamma_o) \qquad\qquad\qquad (4A)$$

29

$$\psi_p = -j \, 1.19 \times 10^6 \, \alpha_e (1 + \Gamma_o) \tag{5A}$$

The magnetic and electric dipole polarizabilities for elliptical apertures are:[14]

$$\alpha_m = \frac{\pi \ell_y^3 [1 - (\ell_x/\ell_y)^2]}{3[K(\varepsilon) - E(\varepsilon)]} \tag{6A}$$

$$\alpha_e = \frac{\pi \ell_y \ell_x^2 (\ell_y^2 - \ell_x^2)}{3[\ell_y^2 E(\varepsilon) - \ell_x^2 K(\varepsilon)]} \tag{7A}$$

where

ℓ_x = 1/2 of the minor elliptical axis

ℓ_y = 1/2 of the major elliptical axis

The terms $K(\varepsilon)$ and $E(\varepsilon)$ are the complete elliptical integrals of the first and second kind respectively:

$$K(\varepsilon) = \int_0^{\pi/2} \frac{d\phi}{\sqrt{1 - \varepsilon^2 \sin^2\phi}} \tag{8A}$$

$$E(\varepsilon) = \int_0^{\pi/2} d\phi \sqrt{1 - \varepsilon^2 \sin^2\phi} \tag{9A}$$

where the eccentricity ε of the ellipse is given by

$$\varepsilon = \sqrt{1 - (\ell_x/\ell_y)^2} \tag{10A}$$

For an elliptical aperture of 0.1 in. $\times$ 0.25 in., the axes are ℓ_x = 0.05 in. and ℓ_y = 0.125 in. Thus ε^2 = 0.840, K = 2.359 and E = 1.151. Therefore

30

$$\alpha_m = \frac{\pi \times (.125 \times .0254)^3 \left[1 - (\frac{.05}{.125})^2\right]}{3 \times [2.359 - 1.151]}$$

$$= 2.329 \times 10^{-8}$$

$$\alpha_e = \frac{\pi \times .125 \times .0254(.05 \times .0254)^2(.125^2 - .05^2)}{3 \times [.125^2 \times 1.151 - .05^2 \times 2.359]}$$

$$= 5.816 \times 10^{-9}$$

From a measurement of σd, the reflection coefficient Γ_o was found from Figure 4 to be -0.88 for the 280 $\overset{o}{A}$ nickel film. Then

$$\psi_m = j \; 1.312 \times 10^6 \times 2.329 \times 10^{-8}(1 + .88)$$

$$= j \; 0.0575$$

$$\psi_p = -j \; 1.19 \times 10^6 \times 5.816 \times 10^{-9}(1 - .88)$$

$$= -j \; 0.000831$$

The thin film with a rectangular aperture with $\ell_y >> \ell_x$ exhibits a capacitive reactance where the same aperture in a foil will exhibit an inductive reactance. The net scattering coefficient is $\psi = (\psi_m + \psi_p)$.

Experimental values of the net scattering coefficient, ψ, have been measured for $\ell_y = 0.5$ inches and are shown in Figure 1A. An effort is now being made to construct a mathematical model for ψ for the rectangular slot.
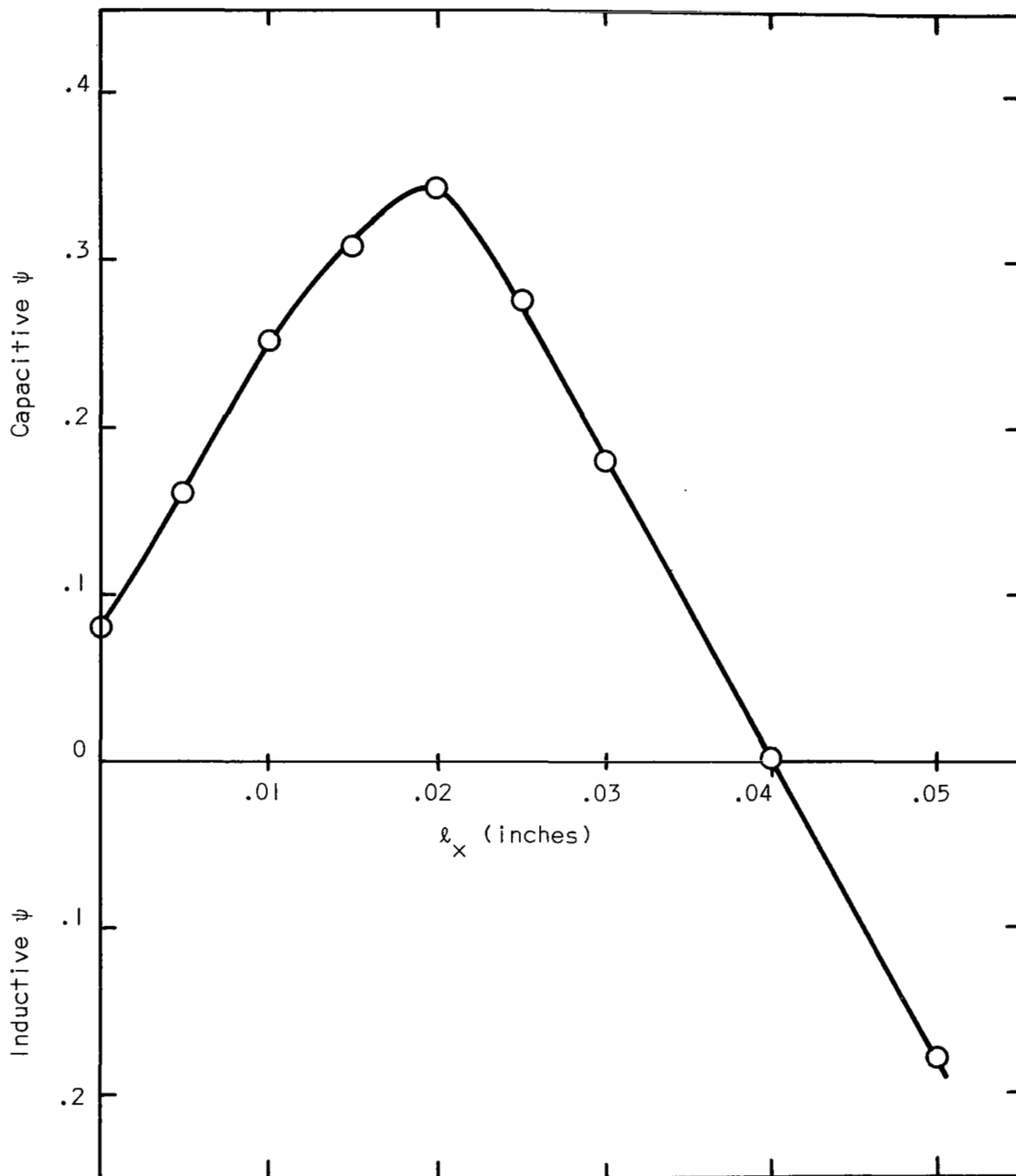
Figure IA. ψ from Experimental Data, 475 Å Nickel Film with Rectangular Aperture, $\ell_y = 0.5$ in.

32

References

(1) Fuchs, K., Proc. Cambridge Phil. Soc. 34, 100 (1938).

(2) Sondheimer, E.H., Phys. Rev. 80, 401 (1950).

(3) _____, Advan. Phys. (Supplement Phil. Mag.) 1, 1 (1952).

(4) Ramey, R. L. and Lewis, T.S., J. Appl. Phys. 39, 1747 (1968).

(5) Ramey, R.L. and Landes, H.S., et. al., J. Appl. Phys. 39, 3883 (1968).

(6) Bethe, H.A., Phys. Rev. 66, 163 (1944).

(7) Bouwkamp, C.J., Phillips Res. Repts., 5, 321 (1950).

(8) Collin, R.E. and Eggimann, W.H., IRE Trans. on Microwave Theory and Techniques, 9, 110 (1961).

(9) Eggimann, W.H., IRE Trans. on Microwave Theory and Techniques, 9, 408 (1961).

(10) Eggimann, W.H. and Collin, R.E., IRE Trans. on Microwave Theory and Techniques, 12, 528 (1964).

(11) See the Detailed Bibliography given in Reference (9).

(12) Collin, R.E., Foundations for Microwave Engineering, McGraw-Hill, New York (1966).

(13) Corson, D.R., and Lorain, P., Introduction to Electromagnetic Fields and Waves, W. H. Freeman and Co., San Francisco, Calif. (1960).

(14) Collin, R.E., Field Theory of Guided Waves, McGraw-Hill, New York, Section 7.3 (1960).

(15) Stratton, J. A., Electromagnetic Theory, McGraw-Hill, New York, 1941.